

# Journal of Materials Chemistry A

Accepted Manuscript



This is an *Accepted Manuscript*, which has been through the Royal Society of Chemistry peer review process and has been accepted for publication.

*Accepted Manuscripts* are published online shortly after acceptance, before technical editing, formatting and proof reading. Using this free service, authors can make their results available to the community, in citable form, before we publish the edited article. We will replace this *Accepted Manuscript* with the edited and formatted *Advance Article* as soon as it is available.

You can find more information about *Accepted Manuscripts* in the [Information for Authors](#).

Please note that technical editing may introduce minor changes to the text and/or graphics, which may alter content. The journal's standard [Terms & Conditions](#) and the [Ethical guidelines](#) still apply. In no event shall the Royal Society of Chemistry be held responsible for any errors or omissions in this *Accepted Manuscript* or any consequences arising from the use of any information it contains.



## Shape-controlled porous heterogeneous PtRu/C/Nafion microspheres enabling high performance direct methanol fuel cells

Received 00th January 20xx,  
Accepted 00th January 20xx

DOI: 10.1039/x0xx00000x  
[www.rsc.org/](http://www.rsc.org/)

Qingqing Cheng,<sup>a,b</sup> Yanlin Wang,<sup>a,b</sup> Jingjing Jiang,<sup>b</sup> Zhiqing Zou,<sup>b\*</sup> Yi Zhou,<sup>b</sup> Jianhui Fang,<sup>a\*</sup> and Hui Yang<sup>b</sup>

Anode catalytic layer for direct methanol fuel cells (DMFCs) with decreased PtRu loading as low as 1.0 mg cm<sup>-2</sup> has been prepared by an electrospray method. The morphology of electrosprayed composite of PtRu/C/Nafion/polyethylene oxide (PEO) is altered from irregular particle to porous microsphere and to nanofiber by adjusting the PEO content. A hybrid structure is assembled by the porous microspheres as the anode catalytic layer for DMFC, leading to a remarkable enhancement in the maximum power density of 35.4 mW cm<sup>-2</sup>, which is ~50% higher than that of conventional one at the same PtRu loading of 1.0 mg cm<sup>-2</sup> and is even comparable to that (31.5 mW cm<sup>-2</sup>) of conventional one at higher PtRu loading of 2.0 mg cm<sup>-2</sup>. Further investigation reveals that the improved performance is mainly attributed to its hierarchical factual structure. In the primary structure, the single microsphere is with well-distributed PtRu/C and fully rich in nanopores and nano-channels, contributing to an increase in the electrochemical active surface area and higher catalyst utilization. In the secondary structure, the micro-sized pathways are formed by the stereoscopic microspheres, contributing to the enhanced mass transport, higher current density and power density.

### Introduction

Over the last decade, direct methanol fuel cell (DMFC) has attracted significant interests as portable power sources due to its unique properties, including high energy density, easy fuel storage, simplicity and convenience<sup>1-3</sup>. Although great progress has been made in the DMFC technology, there are several challenges that have limited its practical applications, such as high cost, low power density, methanol crossover and poor durability<sup>4-6</sup>.

The membrane electrode assembly (MEA) is the most important part in DMFC with the highest impact on power density, durability and cost<sup>7-10</sup>. Generally, the noble metal loading on each side of an MEA is ca. 3–4 mg cm<sup>-2</sup>, which represents 30%~40% of the total cost. To reduce noble metal loading within the MEA, extensive efforts are devoted to enhance the electrocatalytic activities toward decreasing the Pt content in catalyst materials. Recently, there are some meaningful approaches in developing nanostructured catalytic layers, by improving the densities of so-called triple-phase reaction boundary (TPRB) and optimizing the pathways for electron, proton and mass transport<sup>11-18</sup>. Higher MOR catalytic activities have been achieved by using one-dimensional

(1D) nanomaterials (Pt nanowires, carbon nanotubes, etc.) to displace the conventional 0D nanomaterials<sup>19-21</sup>. Similarly, pore-forming templates (magnesium oxide nanoparticles, silica nanoparticles, etc) have been used to control the morphology of the catalytic layer, leading to an increase in the performance at the PtRu loading of 2.0 mg cm<sup>-2</sup><sup>22</sup>. Particularly, soft-lithography<sup>23-25</sup> and other nanotechnology are more and more involved in the construction of new electrodes. A nanofiber network catalytic layer is designed and constructed by electrospinning, and thereby significantly improved the catalyst utilization and mass transport<sup>26-33</sup>.

According to Fick's law, the mass transport on porous media is simultaneously affected by its pore size, porosity and tortuosity. Fig. 1A schematically shows a conventional electrode assembled by PtRu/C/Nafion agglomerates with small pore size and long tortuosity, resulting in the slow mass transport. In order to address these problems, two structural approaches have been explored successfully, that the one is to increase the pore size and porosity by using pore forming agent or sacrificial template (Fig. 1B<sup>22</sup>) and the other is to reduce the tortuosity by using ordered nanowire array (Fig. 1C<sup>34</sup>). However, it is impossible to get the balance of the pore size, porosity and tortuosity by using a simple structure. A hybrid structure is expected which is formed by two types of pores, including the nanopores toward increasing the TPRB densities and the micropores toward enhancing the mass transport (Fig. 1D).

<sup>a</sup> College of Science, Department of Chemistry, Shanghai University, Shanghai, 200444, China.

<sup>b</sup> Shanghai Advanced Research Institute, Chinese Academy of Sciences, Shanghai, 201210, China. Fax: 86-21-20325112; Email: [zouzq@sari.ac.cn](mailto:zouzq@sari.ac.cn)

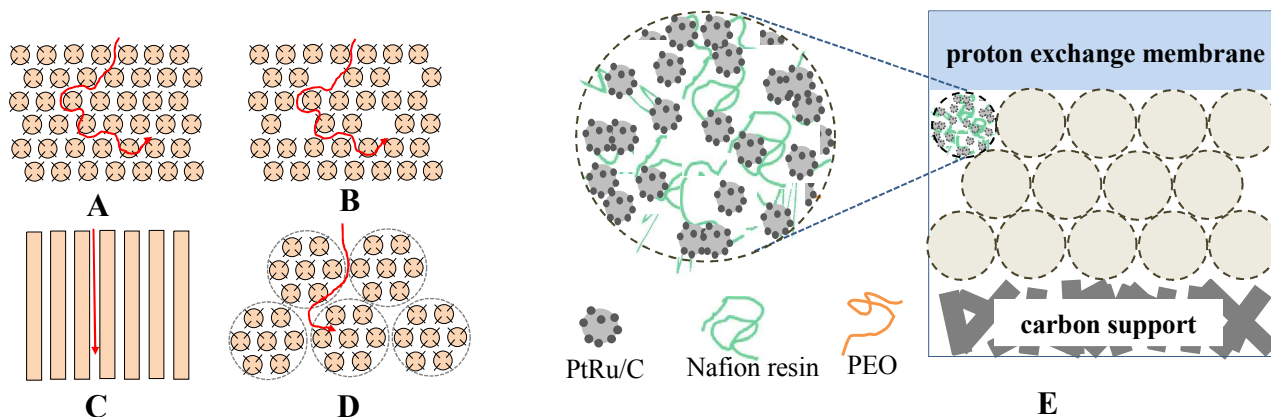


**Fig.1** The schematic diagram of four different catalytic layers and their corresponding mass transport pathways: a conventional electrode (A), an electrode with pore forming agent (B), an electrode in ordered nanowire array (C), an electrode in hybrid structure with porous microspheres (D) and the corresponding anode catalytic layer by using porous PtRu/C/Nafion/PEO microspheres (E)

Electrospray as a very useful technique is used to fabricate different types of particles with diameter ranging from micrometer to nanometer. Herein, the electrospray technique was used to fabricate platinum ruthenium/carbon/Nafion/polyethylene oxide (PtRu/C/Nafion/PEO) microspheres as the porous anode catalytic layer for DMFC (Fig.1E). The microspheres with different morphologies were obtained by adjusting the PEO content, and further evaluated as the anode catalytic layer for DMFC. The morphology, electrochemical performance and relationship between the performance and porous microspheres were investigated. The fabricated porous microspheres were rich in nanopores and nanochannels, which were beneficial for improving the electrochemical surface active area (ESA) and PtRu utilization. The microspheres stacked and formed microchannels, which were favorable for methanol and carbon dioxide transport. The PtRu loading in anode is significantly reduced to as low as half, while the performance is maintained in comparison with the conventional one.

## 19 Experimental Section

### 20 Apparatus and materials

21 PEO (molecular weight, Mw = 300,000) was purchased from Aldrich. 22 Nafion® solution (5 wt.%) was from DuPont Co., USA. PtRu/C (40 wt.% Pt and 20 wt.% Ru) and PtRu (1:1) black were obtained from Johnson Matthey Company. Carbon paper (TGPH060, 20 wt.% polytetrafluoroethylene, PTFE) was from Toray Company. The microporous layer was composed of XC-72R and PTFE with the mass ratio of 4:1. All chemicals were of analytical grade. The homemade electrospinning/electrospraying setup included a high voltage (0–30

29 kV) power source, a syringe pump, a steel needle and an aluminum 30 plate as the ground collector.

### 31 Electrospay fabrication of PtRu/C/ Nafion/PEO microsphere 32 catalytic layer

33 Synthesis of PtRu/C/Nafion/PEO particles, porous microspheres and 34 nanofibers: An electrostray ink was prepared by mixing PEO (0–20 35 mg) into 5 wt.% Nafion solution (1.330 g) by stirring for 2 h, then 36 adding a mixture of PtRu black (166.67 mg) and PtRu/C (55.55 mg, 37 60 wt.%) by stirring for another 2 h. The ink was electrosprayed at a 38 rate of 0.2 ml h<sup>-1</sup> by a syringe pump (KDS 200) with 12 cm grounded 39 collector to the needle at a high voltage of 16 kV at room 40 temperature and at the humidity of 45±5%.

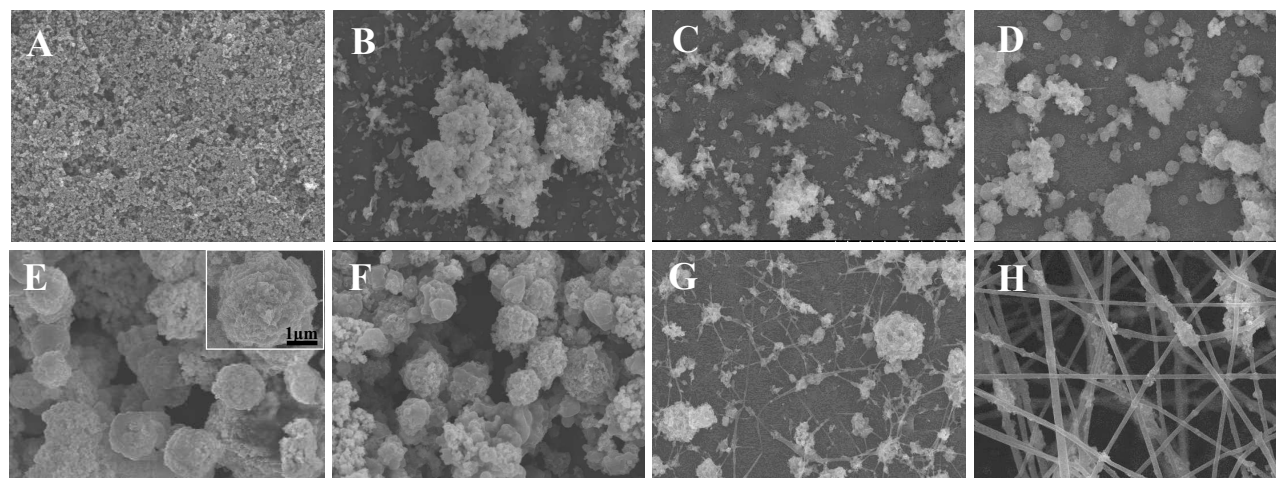
41 The conventional MEA was prepared as before with a 42 Nafion® 115 membrane, a cathode by air brush with a Pt loading of 4 43 mg cm<sup>-2</sup> and an anode by air brush with a PtRu loading of 1~2 mg 44 cm<sup>-2</sup>. The electrosprayed MEA was prepared with the same 45 membrane and cathode, while the anode was displaced with the 46 microsphere catalyst layer with a PtRu loading of 1 mg cm<sup>-2</sup>.

### 47 Morphology and electrochemical characterization of the 48 microspheres

49 Characterization: FESEM images were collected on Field Emission 50 Scanning Electron Microscopy (FESEM, Hitachi S-4800) and TEM 51 image was conducted with Field Emission Transmission Electron 52 Microscopy (FETEM, JEOL 2100F).

53 Cyclic voltammetric (CV) measurements were carried out with 54 a Solatron SI1287 Potentiostat/Galvanostat system to characterize 55 the ESA of the MEAs, by feeding the water to the anode as the 56 working electrode, humidified H<sub>2</sub> to the cathode at a flow rate of 5

## PAPER



2 μm

**Fig. 2.** The SEM images of electrodes fabricated by air brush without PEO (A), and by electro spray with PEO of different contents: 0mg (B), 4mg (C), 8mg (D), 10mg (E, insert, it is SEM image of a single microsphere), 12mg (F), 16mg (G) and 20mg, (H).

1 mL min<sup>-1</sup> as the counter electrode and the reference electrode (dynamic hydrogen electrode, DHE). The working potential was cycled from 0 to 0.7 V and at a scan rate of 20 mV s<sup>-1</sup>.

The ESA of the anode was further checked by CO-stripping method with a Solartron SI1287 Potentiostat/Galvanostat system since it directly denotes the electrocatalytic active sites for methanol oxidation reaction (MOR). Firstly, the anode catalyst layer was completely pre-absorbed with CO for 30 min at the holding potential of 0.2 V. Then, the residual free CO was removed by N<sub>2</sub> for 20 min. Finally, the CO-stripping voltammogram was carried out in the potential range of 0–1.0 V and at a scan rate of 20 mV s<sup>-1</sup> where the anode was fed with N<sub>2</sub> as the working electrode and the cathode was fed with humidified H<sub>2</sub> as the counter and reference electrode.

Electrochemical impedance spectra (EIS) measurements of the anodes were carried out with a Solartron SI1260 and Solartron SI1287 Potentiostat /Galvanostat system. The anode was fed with 4 M methanol solution as the working electrode and cathode was passively fed with oxygen from air as the counter electrode. The EIS measurements were performed at a voltage of 0.4 V with a frequency range from 100 kHz to 0.01 Hz, and at the amplitude of the sinusoidal voltage signal of 10 mV.

### The performance evaluation of the MEAs

The performance of the MEAs was evaluated by polarization tests with an Arbin Fuel Cell Testing System (Arbin Instrument Inc., USA). The as-prepared MEAs with an active surface area of 4 cm<sup>2</sup> were

activated in 2 mol L<sup>-1</sup> methanol solution and measured in a DMFC testing setup. Methanol solution (4 mol L<sup>-1</sup>) was passively fed to the anode by self-transport and the cathode was exposed to the atmosphere (air-breathing mode). All electrochemical tests were performed at a temperature of ca. 25 °C and the humidity of 30–40%. The durability test of the MEA was measured at a constant current discharging of 40 mA cm<sup>-2</sup> with discontinuous feed with 4 mol L<sup>-1</sup> of methanol solution.

## Results and discussion

### Effect of PEO content on the morphology of the electro sprayed catalytic layer

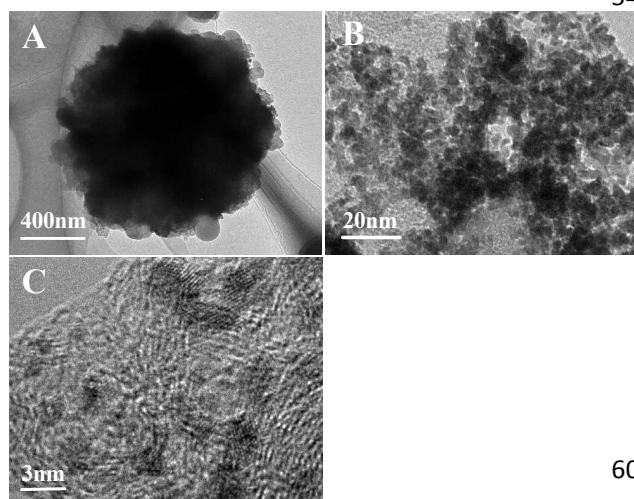
The natural properties of the electro spray ink, including viscosity, polymer concentration, ion concentration and solvent evaporability, are significantly important for the formation of particles and morphology controlling of the catalytic layer. Herein, the PEO is used as the carrier polymer to control the ink viscosity and further to control the morphology of the electro sprayed catalytic layers. Different shapes of particles and fibers are fabricated by varying the PEO content from 0, 4, 8, 10, 12, 16 to 20 mg as shown in Figs. 2B–H. As a comparison, a conventional anode catalytic layer was prepared by airbrush as shown in Fig. 2A. From Figs. 2B, 2C and 2D, small irregular particles are formed at the PEO contents of 0, 4 and 8 mg, because the ink viscosity is too low to form a stable Taylor cone. With an increase in the PEO content to 10 and 12 mg, the irregular particles disappear and porous microspheres with an average diameter of 1–3 μm are formed as

## ARTICLE

Journal Name

1 shown in Figs. 2E and 2F. From the inset of Fig. 2E, the surface of a  
 2 typical microsphere is very rough and there are many deep nano  
 3 sized folds within the microsphere, which can remarkable increase  
 4 the surface area and help more catalyst nanoparticles to be  
 5 exposed. Furthermore, it is a hybrid structure of microsphere and  
 6 fiber when the PEO content is increased to 16 mg (Fig. 2G).  
 7 Continuous nanofibers are fabricated by so called electrospinning,  
 8 when the PEO content is 20 mg (Fig. 2H). Therefore, the  
 9 morphology of the anode catalytic layers, including irregular  
 10 particles, microspheres and nanofibers is facily controlled by ju  
 11 varying the PEO content in the range of 0–20 mg.

12 TEM images show the inner structures of the microsphere.  
 13 typical microsphere is almost of spherical and its surface is ve  
 14 rough in Fig.3A. It is clearly shown the surface of the microsphere  
 15 Fig. 3B, suggesting that the PtRu nanoparticles are al  
 16 individually distributed and there are several nanochannels on the  
 17 surface, which would result in higher ESAs and higher Pt  
 18 utilization. The high-resolution TEM image in Fig. 3C further prov  
 19 that PtRu nanoparticles are well distributed in the electrospayed  
 20 composites and the average diameter is about 2.5 nm.



22 Fig.3. The TEM images of electrospayed microsphere (A, a single  
 23 microsphere; B, the edge of the microsphere; C, the HRTEM image of the  
 24 electrospayed microsphere).

25 The Raman and FT-TR spectra are to reveal the chemical  
 26 structure changes as shown in Fig.4. The Raman spectra with two  
 27 bands of  $1345\text{cm}^{-1}$  and  $1595\text{cm}^{-1}$  can be attributed to the D-band  
 28 and G-band of carbon, respectively. From Fig. 4A, the Raman  
 29 spectra for the two catalytic layers are almost same, implying that  
 30 the carbon structure stays the same after the electrospaying.  
 31 4B shows the FT-IR spectra of the two catalytic layers, where the  
 32 similar vibrating peaks corresponding to the  $-\text{C}-\text{O}-\text{C}$ ,  $-\text{S}-\text{O}$  and  
 33  $-\text{C}-\text{F}$  bonds are attributed to Nafion resin, suggesting that the  
 34 Nafion resin structure maintains unchanged. It should be notice  
 35 that there is no special peaks for PEO, suggesting that the PEO ratio  
 36 is too low to be measured. In brief, there are only physical  
 37 morphology changes and no chemical structure changes after  
 38 electrospaying process.

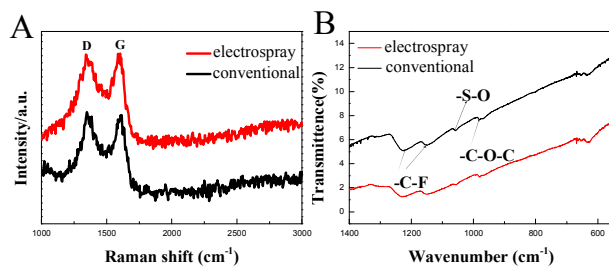


Fig.4. A comparisons of the Raman spectra(A) and FT-IR spectra (B) between the electrospayed catalytic layer and conventional one.

### Performance comparison of the DMFCs with different anode catalytic layers

The porous microspheres were used as the anode catalytic layer and further evaluated by the polarization measurement in DMFCs. The effects of PEO contents on the polarization curves are shown in Fig. 5A. The maximum power densities vary dramatically ( $22.86$ ,  $29.62$ ,  $35.44$ ,  $32.23$ ,  $28.04$  and  $21.01\text{ mW cm}^{-2}$ ) when the PEO content is increased from 4 to 20 mg  $\text{cm}^{-2}$  (The MEA can not be prepared by electrospaying without PEO). Corresponding to the PEO content of  $\sim 10\text{ mg}$ , the DMFC exhibits the best power density of  $35.44\text{ mW cm}^{-2}$ , which confirms that the microspheres are more promising as the structure for anode catalytic layer than the others (irregular particle and nanofiber).

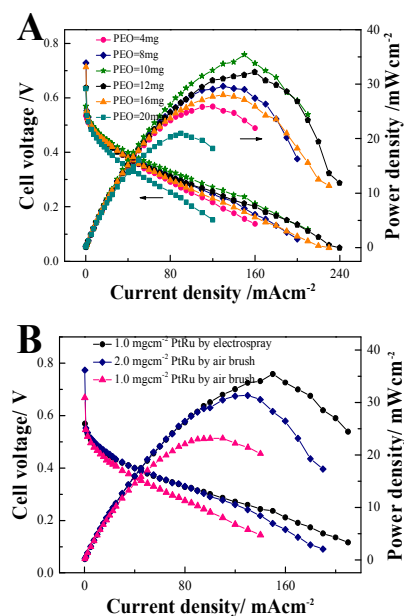


Fig.5. The steady-state polarization curves of the DMFCs with electrospayed anode with different PEO content at PtRu loading of  $1.0\text{ mg cm}^{-2}$  (A), and the comparison of the polarization steady-state polarization curves of the DMFCs with electrospayed anode and the airbrushed anode at different PtRu loadings (B).

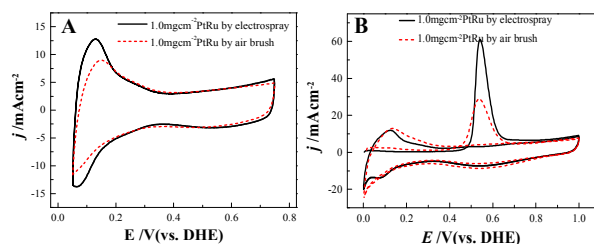
The DMFC performance was also compared by the polarization curves as shown in Fig. 5B, where the DMFC with electrospayed anode was at a PtRu loading of  $1.0\text{ mg cm}^{-2}$  (curve a) and that with

1 conventional anode was at a PtRu loading of 1.0 mg cm<sup>-2</sup> (curve 46  
2 and 2.0 mg cm<sup>-2</sup> (curve c). The maximum power density of DMFC 47  
3 electro spray can reach to about 35.4 mW cm<sup>-2</sup>, which was 50  
4 higher than that (23.5 mW cm<sup>-2</sup>) by airbrush at the same Pt 49  
5 loading and was even comparable to that (31.5 mW cm<sup>-2</sup>) 50  
6 airbrush at double PtRu loading. Importantly, the PtRu loading 51  
7 could be dramatically reduced to half of the conventional one 52  
8 using this porous microsphere structure. From the SEM images 53  
9 shown in Figs. 2E and 2A, the surface of electro sprayed anode 54  
10 extremely rough and the average diameter of the channels formed 55  
11 by the microspheres is 1~3 μm, thus leading to almost free mass 56  
12 transport. However, the surface of the conventional anode was 57  
13 smooth and the average diameter of the channels between the 58  
14 nanoparticles was only about tens of nanometers, thus leading to 59  
15 sluggish mass transport. Therefore, the performance improvement 60  
16 by using the electro sprayed anode can be attributed to its fine 61  
17 pathways for mass transport.

## 18 Electrochemical measurement

### 19 Analysis of the ESA by CVs and CO-stripping voltammogram

20 To explore the possible reasons for the improved performance 65  
21 the DMFCs, the CVs and CO-stripping voltammograms 66  
22 measurements were carried out to compare the ESAs of the anode 67  
23 catalytic layers with different morphology as shown in Figs. 6A and 68  
24 6B, respectively. The redox peaks in the potential range 0.05–0.4 V 69  
25 can be ascribed to the absorption and desorption of hydrogen 70  
26 the surface of PtRu particles. ESA is calculated quantitatively by the 71  
27 equation:  $ESA = Q_H/m \times C$ , where  $Q_H$  is the charge for hydrogen 72  
28 desorption (mC cm<sup>-2</sup>);  $m$  is the amount of Pt loading (mg cm<sup>-2</sup>);  $C$  is 73  
29 the charge required to oxidize a monolayer of hydrogen on Pt (0.21 74  
30 mC cm<sup>-2</sup>) after subtracting the charge caused by the electric double 75  
31 layer. The calculated ESA by hydrogen adsorption of the anodes 76  
32 electro spray and by airbrush at PtRu loading of 1.0 mg cm<sup>-2</sup> were 77  
33 27.27 and 18.03 m<sup>2</sup> g<sup>-1</sup>, respectively. The ESA in electro sprayed 78  
34 anode increases by ~50%, indicating a significant improvement 79  
35 catalyst utilization of the anode catalytic layer fabricated 80  
36 electro spray. 81  
37



38 **Fig. 6.** CVs (A) and CO-stripping voltammograms (B) of electro sprayed anode 82  
39 and air brushed anode with the PtRu loading of 1.0 mg cm<sup>-2</sup>. 83  
40

41  
42 For PtRu (1:1, atom ratio) alloy catalyst, the ESA by 95  
43 adsorption is only for Pt in the PtRu catalysts and that by 96  
44 stripping are for both Pt and Ru in the PtRu catalysts. Hence, the 97  
45 calculation of CO-stripping can more accurately display the MOR 98

sites of the PtRu nanoparticles. Fig. 6B clarified that the calculated 99  
ESA by CO-stripping of electro sprayed anode was 53.37 m<sup>2</sup> g<sup>-1</sup>, 100  
which was almost twice that of the conventional one (27.91 m<sup>2</sup> g<sup>-1</sup>). 101  
The notable increase in the ESA is mainly attributed to its highly 102  
porous structure of the microspheres, which is in good agreement 103  
with the morphology results. Moreover, high ESA is also attributed 104  
to the well-distribution of the PtRu nanoparticles and the enhanced 105  
interactions among the catalysts and ionomer. 106

### 107 Analysis of the anodes by the EIS

108 EIS can help to understand the mechanisms of the oxidation of the 109  
DMFC under actual operating conditions, by comparing the effects 110  
of reaction resistance, charge transfer resistance and mass 111  
transport resistance. Fig. 7 shows the comparison of the results of 112  
the EIS of the DMFCs with electro sprayed anode and conventional 113  
anode, respectively, at the PtRu loading of 1.0 mg cm<sup>-2</sup>. 114  
Corresponding equivalent circuit model is shown in Fig. 7. The 115  
constant phase element (CPE) is considered as the current 116  
capacities including the Faraday current and charging current as a 117  
non-uniform structure of porous electrodes. Therefore, the physical 118  
meanings of each element used in the equivalent circuit model are 119  
as follows: 120

Where  $R_m$  denotes the resistance of membrane;

$CPE_i$  and  $R_i$  display the properties of the anode membrane 121  
interface including the capacitive behavior and interface resistance 122  
between the catalytic layer and the Nafion membrane, respectively. 123

$R_{ct}$  is the charge-transfer resistance of the electrode reaction;

$CPE_d$  is the capacitive behavior of the catalytic layer with 124  
roughness of the catalytic layer and non-uniform catalyst 125  
distribution. 126

$R_c$  and  $L_{co}$  are the current signal following the voltage 127  
perturbation with a phase-delay due to coverage change of the 128  
intermediate  $CO_{ad}$  in the anode catalytic layer because the 129  
oxidation of the  $CO_{ad}$  is the rate-limiting step for DMFC. 130

The fitted parameters are listed in Table 1. Comparison of the 131  
DMFCs with the conventional anode and electro sprayed anode, 132  
respectively, indicated the occurrence of an obvious smaller arc for 133  
DMFC with the electro sprayed anode at the middle-frequency 134  
region, resulting in a significant decrease in the values of  $R_c$ ,  $L_{co}$ , 135  
and  $R_{ct}$ . The reduced values of  $R_c$  and  $L_{co}$  indicate that the 136  
oxidation reaction rate of the intermediate (Pt active site)-CO is 137  
more rapid and efficient, attributed to its high ESA and rapid 138  
transport of the product  $CO_2$  by the new structure. The decreased 139  
value of  $R_{ct}$  is due to its high ESA, uniform distribution and efficient 140  
pathways for electron and proton transport. As a consequence, 141  
there is corresponding relationship between the parameter changes 142  
in the EIS analysis with the structural changes in the physical and 143  
electrochemical evaluations. 144

### 145 The energy conversion efficiency and durability measurements

146 To explore the energy conversion efficiency and durability, Fig. 8 147  
shows the corresponding discharging curves at constant voltage 148  
(0.35 V) and constant current (160 mA) of the DMFCs with different 149  
anodes by feed with 4 mL of 4 mol L<sup>-1</sup> methanol solution. The 150

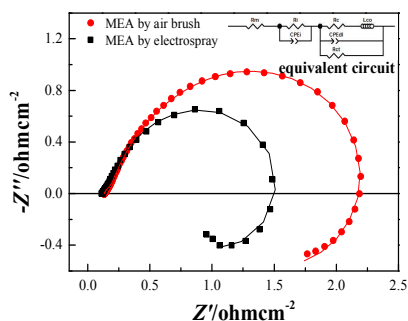


**Fig. 7.** Electrochemical impedance spectra (Insert, the equivalent circuit) of the anodes of the two MEAs with the anodic catalytic layers fabricated by air brush and electro spray with a PtRu (1:1) loading of  $1.0 \text{ mg cm}^{-2}$  at a given DC potential of 0.4 V.

**Table 1** Fitting parameters for the CPE-based equivalent circuit models for the anodes at 0.4 V and at  $25^\circ\text{C}$ .

Parameter	GDE anode ( $1 \text{ mg cm}^{-2}$ )	Electro spray anode ( $1 \text{ mg cm}^{-2}$ )
Rm	0.53	0.46
Ri	0.19	0.23
CPEi-T	0.21	0.22
CPEi-P	0.83	0.80
Rc	4.31	2.33
Lco	89.90	32.22
CPEd-T	0.29	0.27
CPEd-P	0.82	0.87
Rct	11.35	6.86

energy conversion efficiency of the DMFCs with conventional anode and electro sprayed anode were 13.24 and 18.42%, respectively, indicating that the energy conversion efficiency was improved significantly when using the microsphere structure. Fig. 8 also demonstrated that the discharging current of the DMFC with electro sprayed anode is much higher than that of the conventional one during the first 20 h, indicating that the formation of porous microspheres can obviously improve the electrocatalytic activity. From a 120 h durability testing of the DMFC as shown in the inset of Fig. 8, the discharging voltage keeps at ca. 0.35 V with some fluctuation at a given current density of  $40 \text{ mA cm}^{-2}$ , confirming the durability of such a DMFC is good for the practical application with an improved cell performance. The voltage fluctuation may be due to the water flooding at cathode side and to the possible change in methanol concentration during the test.

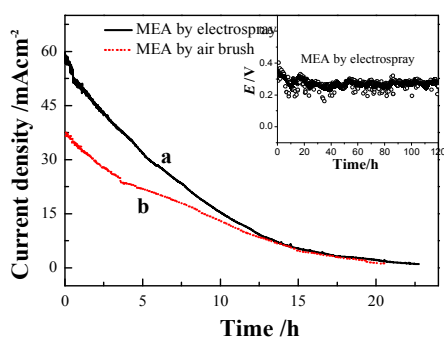


**Fig. 8.** The energy conversion efficiency measurements of DMFCs with electro sprayed anode (a) and air brush anode (b) at the PtRu loading of  $1.0 \text{ mg cm}^{-2}$ . Insert: the stability of a DMFC with electro sprayed catalytic layer of  $1.0 \text{ mg cm}^{-2}$  PtRu and at a constant current of 160 mA.

## 31 Conclusions

A structure of porous microspheres was successfully designed, fabricated and applied as the anode catalytic layer for DMFC, which can result in a significant decrease in the PtRu loading and enhancement in the DMFC's performance. This hierarchical factual structure with micropores for enhancing the mass transport and nanopores for increasing the PtRu utilization could be responsible for the improved performance. The usage and the content change of PEO is the key factor in forming the shape-controlled microspheres. This technology could provide a simple and promising way to fabricate shape-controlled porous hybrid catalytic layers, thus significantly improving the catalyst utilization and decreasing the noble metal loading in fuel cell.

## 44 Acknowledgements

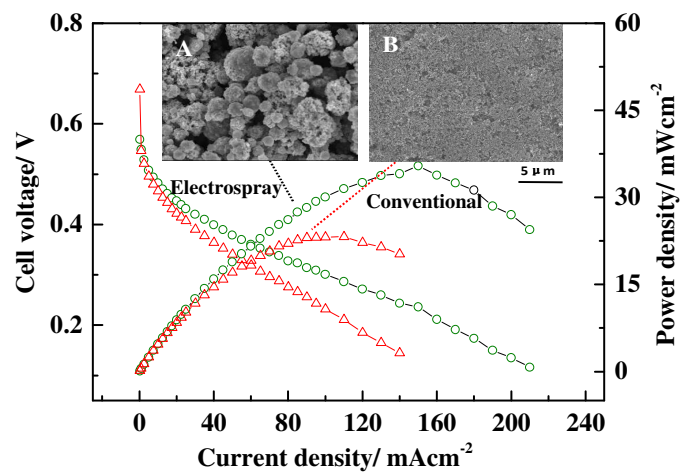
We would like to thank the National High-tech R&D Program (863 Program, 2015AA043503), National Basic Research Program of China (973 Program, 2012CB932800), Nature Science Foundation of China (21373256), Science and Technology Commission Shanghai Municipality (15ZR1415100) for support to this work.

## 50 Notes and references

- 1 R. Chen, T. S. Zhao, *J. Power Sources*, 2005, **152**, 122–130.
- 2 S. Eccarius, X. Tian, F. Krause, C. Agert, *J. Micromech. Microeng.*, 2008, **18**, 104010–104018.
- 3 X. Li, A. Faghri, *J. Power Sources*, 2013, **226**, 223–240.
- 4 M. Winter, R. J. Brodd, *Chem. Rev.*, 2004, **101**, 4245–4270.
- 5 C. M. Miesse, W. S. Jung, K. J. Jeong, J. K. Lee, J. Lee, J. Han, S. P. Yoon, S. W. Nam, T. H. Lim, S. A. Hong, *J. Power Sources*, 2006, **162**, 532–540.
- 6 A. S. Aricò, S. Srinivasan, V. Antonucci, *Fuel Cells*, 2001, **1**, 133–161.
- 7 M. Y. Li, S. Z. Zhao, G. Y. Han, B. S. Yang, *J. Power Sources*, 2009, **191**, 351–356.
- 8 G.-H. An, H.-J. Ahn, *J. Electroanal. Chem.*, 2013, **707**, 74–77.
- 9 H. Joh, S. Hwang, J. Cho, T. Ha, S. Kim, S. Moon, H. Ha, *Int. J. Hydrogen Energy*, 2008, **33**, 7153–7162.
- 10 H. Wu, H. Zhang, *J. Power Sources*, 2014, **248**, 1264–1269.
- 11 H. J. Kim, W. B. Kim, *Electrochem. Commun.*, 2010, **12**, 32–35.
- 12 Y. Bi, G. Lu, *Chem. Mater.*, 2008, **20**, 1224–1226.
- 13 H. Yang, *Angew. Chem. Int. Ed.*, 2011, **50**, 2674–2676.
- 14 J. X. Wang, H. Inada, L. Wu, Y. Zhu, Y. Choi, P. Liu, W. P. Zhou, R. Adzic, *J. Am. Chem. Soc.*, 2009, **131**, 17298–17302.
- 15 X. G. Wang, J. H. Liao, C. P. Liu, W. Xing, T. H. Lu, *Electrochem. Commun.*, 2009, **11**, 198–201.

- 1 16 Z. Y. Bai, L. Yang, L. Li, J. Lv, K. Wang, J. Zhang, *J. Phys. Chem. C*,  
2 2009, **113**, 10568–10573.
- 3 17 L. Michal, S. Tali, V. Alexander, R. Israel, *Angrew. Chem. Int. Ed*,  
4 2003, **42**, 5576–5579.
- 5 18 D. H. Lee, W. J. Lee, W. J. Lee, S. O. Kim, Y. H. Kim, *Phys. Rev.*  
6 *Lett*, 2011, **106**, 175502–175505.
- 7 19 M. T. Sung, M. H. Chang, *J. Power. Sources*, 2014, **248**, 320–326.
- 8 20 J. Y. Cao, C. Du, S. C. Wang, P. Mercier, X. G. Zhang, H. Yang, D.L.  
9 Akins, *Electrochem. Commun*, 2007, **9**, 735–740.
- 10 21 M. Hezarjaribi, M. Jahanshahi, *Appl. Surf. Sci.*, 2014, **295**,  
11 144–149.
- 12 22 Q. Huang, Hui Yang, *J. Power Sources*, 2014, **262**, 213–218.
- 13 23 Y. N. Xia, G. M. Whitesides, *Annu. Rev. Mater. Sci.*, 1998, **28**,  
14 153–84.
- 15 24 H. T. Ng, M. L. Foo, J. Li, S. F. Y. Li, *Langmuir*, 2002, **18**, 1-5.
- 16 25 F. Qian, Z. He, Y. Li, *Bioresource Technol*, 2011, **102**, 5836–5840.
- 17 26 S. Cavaliere, S. Subianto, I. Savych, *Energy Environ. Sci.*, 2011, **4**,  
18 4761–4785.
- 19 27 J. Shui, James C.M.Li, *Nano Lett.*, 2009, **4**, 1304–1314.
- 20 28 J. Shui, James C.M.Li, *Adv. Funct. Mater.*, 2011, **21**, 3357–3362.
- 21 29 D. C. Higgins, R. Wang, Z. Chen, *Nano Energy*, 2014, **10**, 135–143.
- 22 30 M-T. Sung, M-H .Chang, *J. Power Soureecs*, 2014, 249, 320–326.
- 23 31 J. Shui, J Zhang, *J. Mater. Chem.*, 2011, **21**, 6225–6229.
- 24 32 J. Wu, Q. Du, H. Yang, *ACS Catal*, 2014, **4**, 144-15.
- 25 33 P. Chen, Z. Zou, *J. Power Sources*, 2014, **255**, 71–74.
- 26 34 A. K. Schmoeckel, M. K. Debe, *J. Power Sources*, 2006, **161**,  
27 1002–1011.
- 28

Colour graphic:



Electrospray porous heterogeneous PtRu-C/Nafion/PEO microsphere as the anode catalytic layer for direct methanol fuel cells with enhanced performance.